

# Excitations of $2_1^+$ and $3_1^-$ states from $(p, p')$ and electromagnetic measurements

M. A. Kennedy, P. D. Cottle, and K. W. Kemper

*Department of Physics, Florida State University, Tallahassee, Florida 32306*

(Received 20 July 1992)

A reanalysis of  $(p, p')$  data taken on  $2_1^+$  and  $3_1^-$  states of 37 even-even  $A \geq 40$  nuclei at energies of  $E < 50$  MeV has been performed with a consistent procedure involving coupled-channels calculations and Becchetti-Greenlees optical model parameters. The matrix elements extracted from this analysis have been compared to matrix elements deduced from electromagnetic measurements of the same excitations. It is concluded that the differences between  $(p, p')$  and electromagnetic results which are often observed do *not* result from variations in the method of analysis of the  $(p, p')$  data. Instead, the differences are caused by experimental errors and nuclear structure effects. The nuclear structure effects are examined by extracting the ratios  $M_n/M_p$  of the neutron and proton multipole matrix elements for both the  $2_1^+$  and  $3_1^-$  states from the proton and electromagnetic data.

PACS number(s): 21.60.Ev, 25.40.Ep, 23.20.Js

## I. INTRODUCTION

Much of the work in the field of nuclear structure has focused on electric quadrupole and octupole collectivity. A great deal of information regarding such collective behavior has been extracted from measurements of the electromagnetic matrix elements linking  $2^+$  and  $3^-$  states to the ground states of even-even nuclei. There are a number of methods for determining these matrix elements directly, including Coulomb excitation, inelastic electron scattering, and lifetime measurements. However, the method of proton inelastic scattering, in which the interaction between proton and target nucleus is dominated by the nuclear force and *not* the electromagnetic force, has also been used for estimating electromagnetic matrix elements. To extract such estimates, the angular distributions of scattered protons are generally analyzed using the distorted wave Born approximation (DWBA) or coupled channels with a form factor which assumes either vibrational or rotational behavior. The analysis gives a deformation parameter  $\beta_L$ , which then yields what Bernstein [1] called  $G_L$ .  $G_L$  has often been used as an estimate for the reduced electromagnetic matrix element  $B(EL; 0_{g.s.}^+ \rightarrow L)$ .

Spear [2] investigated the correspondence between  $G_3$  and electromagnetic matrix elements  $B(E3; 0_{g.s.}^+ \rightarrow 3_1^-)$  in even-even nuclei by comparing them in nuclei where both  $(p, p')$  and electromagnetic measurements are available. Spear calculated the ratio

$$H = \frac{G_3}{B(E3; 0_{g.s.}^+ \rightarrow 3_1^-)} \quad (1)$$

for 51 nuclei having  $A > 20$ , and found that  $H$  has a mean value of 1.01 and a standard deviation  $\sigma_H$  of 0.36 for these nuclei. For his comparison, Spear used the  $\beta_3$  values reported by the authors of each  $(p, p')$  study without regard to the variations in the completeness of the angular distribution data sets and variations in the methods of analysis. Spear suggested that the scatter of  $H$  values might be partially caused by the variety of methods

used for the analysis of  $(p, p')$  data, and that a smaller standard deviation for  $H$  might be obtained by carefully reanalyzing each  $(p, p')$  experiment using a consistent approach.

In making estimates of electromagnetic matrix elements from  $(p, p')$  results, it is assumed that protons and electromagnetic probes interact with protons and neutrons in the nucleus in the same way. However, it is well known that this is not so: Electromagnetic probes see only the protons in the nucleus, and incident low-energy (10–50 MeV) protons interact more strongly with neutrons in the nucleus than with other protons [3]. These characteristics of the different probes have been used [3] to obtain information about the differences between the oscillations of proton and neutron fluids in  $2_1^+$  states of even-even nuclei.

In this work, we report on an extensive reanalysis of  $(p, p')$  data for  $3_1^-$  states in 30 nuclei with  $A \geq 40$ . For this analysis, a consistent coupled-channels formalism (using the computer code CHUCK [4]) and Becchetti-Greenlees optical model parameters [5] were used for all nuclei. The results of this reanalysis are used to recalculate  $H$  values. The distribution of these new  $H$  values is then compared to Spear's result. In addition, a reanalysis of  $(p, p')$  data on  $2_1^+$  states in 37  $A \geq 40$  nuclei is reported, and the distributions of  $H$  values for  $2_1^+$  and  $3_1^-$  states are compared. Finally, we use the  $(p, p')$  results to look for differences in proton and neutron fluid motion in  $2_1^+$  and  $3_1^-$  states using the analysis described in Ref. [3].

## II. CONSISTENT REANALYSIS OF $(p, p')$ DATA

As Spear suggested, we have emphasized consistency in constructing a procedure for reanalyzing  $(p, p')$  data. The optical parameters needed to generate the entrance and exit channel distorted waves were taken from the global analysis of Becchetti and Greenlees [5]. Since they limited their analysis to the mass region  $A \geq 40$ , we have done so also. In addition, the Becchetti-Greenlees analysis was limited to proton energies less than 50 MeV, and

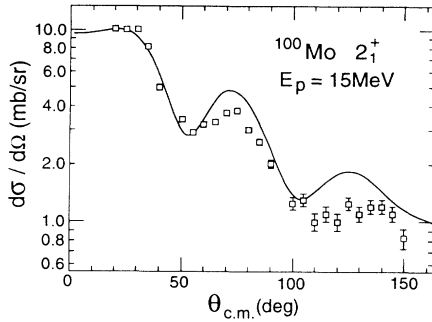


FIG. 1. Experimental and calculated angular distributions for the  $2_1^+$  state in the  $^{100}\text{Mo}(p, p')$  reaction at 15 MeV. The data are taken from [31], and the calculations are performed according to the procedure described in the text.

we have restricted our study to these energies. We have also not considered data taken with beam energies of less than 14 MeV.

As was the case for Spear's compilation, we have not attempted to be exhaustive in our selection of data. Instead, we have attempted to select a representative sample of data. Our decision regarding whether to analyze a particular data set depended in part on whether enough forward angle data were taken to allow a good fit in our analysis.

Instead of the common distorted wave Born approximation (DWBA) approach for generating calculated angular distributions, we have adopted a slightly more sophisticated coupled-channels approach, and have used the computer code CHUCK [4] for our calculations. The  $\beta_L$  values are defined for the usual collective potential  $\beta_L \delta U_{\text{opt}} / \delta r$ . In our procedure, only the coupling between the ground state and the specific excited state being analyzed (either  $2_1^+$  or  $3_1^-$ ) is considered. In extracting a  $\beta_L$  value for each  $(p, p')$  angular distribution (taken from [6–42]), we emphasized fitting the most forward maximum, since the smaller differential cross section at larger angles is often significantly affected by small components in the state's wave function. Examples of our fits to  $2_1^+$  and  $3_1^-$  states in several nuclei are shown in Figs. 1–4.

Experimental errors are often not reported for  $(p, p')$

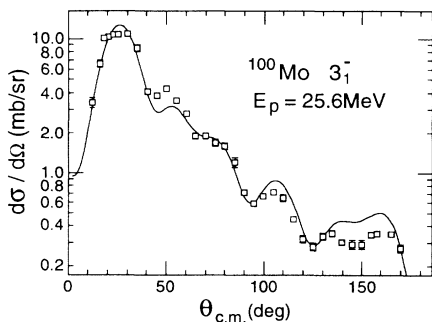


FIG. 2. Experimental and calculated angular distributions for the  $3_1^-$  state in the  $^{100}\text{Mo}(p, p')$  reaction at 25.6 MeV. The data are taken from [32], and the calculations are performed according to the procedure described in the text.

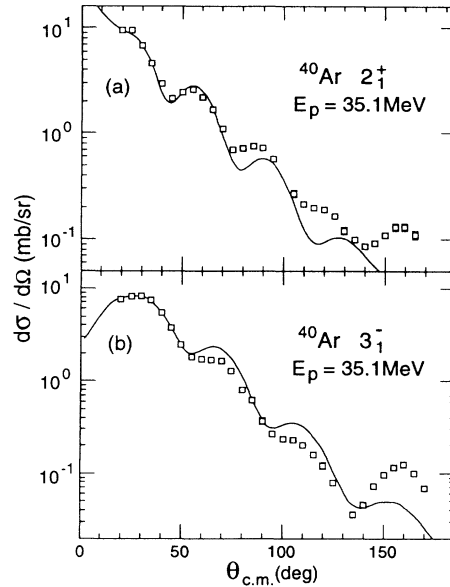


FIG. 3. Experimental and calculated angular distributions for the (a)  $2_1^+$  state and (b)  $3_1^-$  state in the  $^{40}\text{Ar}(p, p')$  reaction at 35.1 MeV. The data are taken from [6], and the calculations are performed according to the procedure described in the text.

results; however, it is important for the analyses in Secs. III and IV that we make reasonable estimates of errors for the  $\beta_L$  values. Because we focused our study on data sets of similar quality, we found that the uncertainties in our  $\beta_L$  results are approximately 7.5% in all

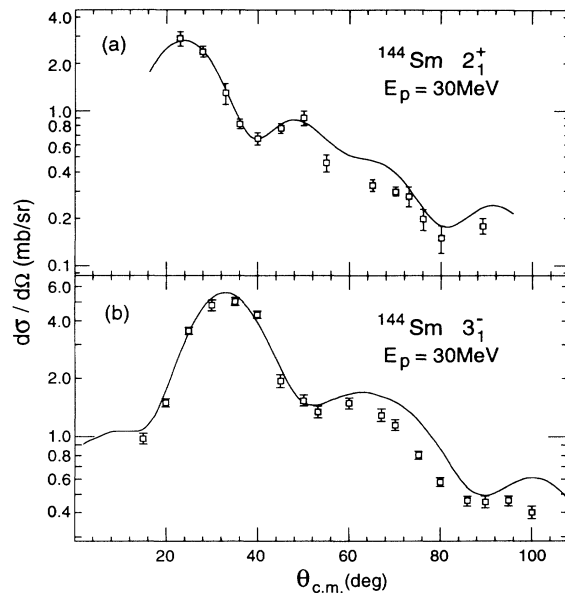


FIG. 4. Experimental and calculated angular distributions for the (a)  $2_1^+$  state and (b)  $3_1^-$  state in the  $^{144}\text{Sm}(p, p')$  reaction at 30 MeV. The data are taken from [36], and the calculations are performed according to the procedure described in the text.

TABLE I. Results of analysis of  $(p, p')$  data for  $2_1^+$  states.

| Nucleus          | $E_{\text{beam}}$ (MeV) | Ref. | $\beta_2^a$ | $G_L$ (W.u.) <sup>b</sup> | Nucleus           | $E_{\text{beam}}$ (MeV) | Ref. | $\beta_2^a$ | $G_L$ (W.u.) <sup>b</sup> |
|------------------|-------------------------|------|-------------|---------------------------|-------------------|-------------------------|------|-------------|---------------------------|
| $^{40}\text{Ar}$ | 29.6                    | 6    | 0.230       | 6.8                       | $^{70}\text{Zn}$  | 22.0                    | 23   | 0.240       | 20.6                      |
| $^{40}\text{Ar}$ | 35.1                    | 6    | 0.242       | 7.5                       | $^{70}\text{Ge}$  | 22.0                    | 24   | 0.250       | 25.5                      |
| $^{40}\text{Ar}$ | 16.9                    | 7    | 0.242       | 7.5                       | $^{72}\text{Ge}$  | 22.0                    | 24   | 0.260       | 27.5                      |
| $^{40}\text{Ar}$ | 14.1                    | 7    | 0.242       | 7.5                       | $^{74}\text{Ge}$  | 22.0                    | 24   | 0.280       | 31.9                      |
| $^{40}\text{Ca}$ | 17.3                    | 7    | 0.140       | 3.1                       | $^{76}\text{Ge}$  | 22.0                    | 24   | 0.250       | 25.5                      |
| $^{40}\text{Ca}$ | 35.0                    | 8    | 0.110       | 1.9                       | $^{88}\text{Sr}$  | 20.2                    | 25   | 0.110       | 6.9                       |
| $^{40}\text{Ca}$ | 30.0                    | 8    | 0.110       | 1.9                       | $^{88}\text{Sr}$  | 19.5                    | 26   | 0.130       | 9.7                       |
| $^{40}\text{Ca}$ | 25.0                    | 8    | 0.110       | 1.9                       | $^{90}\text{Zr}$  | 25.0                    | 27   | 0.088       | 4.9                       |
| $^{40}\text{Ca}$ | 40.0                    | 8    | 0.110       | 1.9                       | $^{90}\text{Zr}$  | 18.8                    | 28   | 0.080       | 4.1                       |
| $^{40}\text{Ca}$ | 14.6                    | 7    | 0.130       | 2.7                       | $^{92}\text{Zr}$  | 40.0                    | 29   | 0.100       | 6.4                       |
| $^{42}\text{Ca}$ | 22.9                    | 9    | 0.215       | 7.4                       | $^{94}\text{Zr}$  | 19.4                    | 30   | 0.125       | 9.9                       |
| $^{44}\text{Ca}$ | 17.5                    | 10   | 0.240       | 9.2                       | $^{92}\text{Mo}$  | 15.0                    | 31   | 0.105       | 7.7                       |
| $^{50}\text{Ti}$ | 40.0                    | 11   | 0.160       | 4.9                       | $^{94}\text{Mo}$  | 25.6                    | 32   | 0.170       | 20.3                      |
| $^{50}\text{Ti}$ | 17.5                    | 12   | 0.180       | 6.2                       | $^{94}\text{Mo}$  | 15.0                    | 31   | 0.160       | 18.0                      |
| $^{50}\text{Ti}$ | 18.2                    | 13   | 0.170       | 5.6                       | $^{96}\text{Mo}$  | 25.6                    | 32   | 0.190       | 25.3                      |
| $^{52}\text{Cr}$ | 17.5                    | 14   | 0.185       | 7.8                       | $^{96}\text{Mo}$  | 15.0                    | 31   | 0.200       | 28.1                      |
| $^{52}\text{Cr}$ | 40.0                    | 11   | 0.160       | 5.9                       | $^{98}\text{Mo}$  | 15.0                    | 31   | 0.175       | 21.5                      |
| $^{52}\text{Cr}$ | 17.5                    | 12   | 0.200       | 9.2                       | $^{98}\text{Mo}$  | 14.7                    | 33   | 0.180       | 22.7                      |
| $^{54}\text{Fe}$ | 40.0                    | 15   | 0.150       | 6.0                       | $^{100}\text{Mo}$ | 25.6                    | 32   | 0.196       | 27.0                      |
| $^{54}\text{Fe}$ | 19.0                    | 16   | 0.160       | 6.9                       | $^{100}\text{Mo}$ | 15.0                    | 31   | 0.250       | 43.9                      |
| $^{54}\text{Fe}$ | 50.0                    | 17   | 0.155       | 6.5                       | $^{116}\text{Sn}$ | 24.5                    | 34   | 0.155       | 23.9                      |
| $^{54}\text{Fe}$ | 17.9                    | 13   | 0.160       | 6.9                       | $^{118}\text{Sn}$ | 24.5                    | 34   | 0.150       | 22.4                      |
| $^{56}\text{Fe}$ | 17.5                    | 14   | 0.290       | 22.6                      | $^{120}\text{Sn}$ | 24.5                    | 34   | 0.140       | 19.5                      |
| $^{58}\text{Ni}$ | 39.7                    | 18   | 0.148       | 6.8                       | $^{120}\text{Sn}$ | 30.0                    | 35   | 0.140       | 19.5                      |
| $^{60}\text{Ni}$ | 19.0                    | 16   | 0.250       | 19.5                      | $^{122}\text{Sn}$ | 24.5                    | 34   | 0.140       | 19.5                      |
| $^{62}\text{Ni}$ | 19.0                    | 16   | 0.250       | 19.5                      | $^{124}\text{Sn}$ | 24.5                    | 34   | 0.140       | 19.5                      |
| $^{64}\text{Zn}$ | 15.0                    | 19   | 0.290       | 31.1                      | $^{138}\text{Ba}$ | 30.0                    | 36   | 0.069       | 5.9                       |
| $^{64}\text{Zn}$ | 22.0                    | 20   | 0.300       | 32.2                      | $^{140}\text{Ce}$ | 30.0                    | 37   | 0.062       | 5.1                       |
| $^{64}\text{Zn}$ | 26.0                    | 21   | 0.340       | 41.4                      | $^{144}\text{Sm}$ | 30.0                    | 38   | 0.079       | 9.5                       |
| $^{64}\text{Zn}$ | 30.0                    | 22   | 0.270       | 26.1                      | $^{144}\text{Sm}$ | 30.0                    | 36   | 0.077       | 9.1                       |
| $^{66}\text{Zn}$ | 22.0                    | 20   | 0.260       | 24.2                      | $^{208}\text{Pb}$ | 40.0                    | 39   | 0.075       | 15.0                      |
| $^{68}\text{Zn}$ | 22.0                    | 23   | 0.240       | 20.6                      | $^{208}\text{Pb}$ | 35.0                    | 40   | 0.060       | 9.6                       |

<sup>a</sup>The errors for  $\beta_3$  are 7.5%.

<sup>b</sup>Calculated from  $\beta_3$  using Eq. (3). The errors for  $G_L$  are 15%.

the cases we studied. Therefore, we adopted this as the error for all of our results.

Once the  $\beta_L$  value is extracted, it must be converted to  $G_L$ . In the present discussion, we have chosen to use one of the prescriptions given by Bernstein [1],

$$G_L = (Z\beta_L)^2(3 + L)^2/4\pi(2L + 1), \quad (2)$$

where  $G_L$  is in single-particle units. A uniform sharp-edge mass distribution with the nuclear radius  $R = (1.20 \text{ fm})A^{1/3}$  is assumed in formulating Eq. (2). While the uniform sharp-edge mass distribution is not strictly correct, it gives a good approximation of nuclear moments for low multipolarities.

Table I lists the  $\beta_2$  and  $G_2$  results of fits to  $2_1^+$  states, and Table II lists the corresponding quantities for  $3_1^-$  states.

### III. COMPARISON OF $G_L$ AND ELECTROMAGNETIC $B(E2)$ AND $B(E3)$ VALUES

The distributions of  $H$  values for  $2_1^+$  and  $3_1^-$  states are shown in Figs. 5 and 6, respectively. In calculating

the  $H$  values, we have followed the same procedure as Spear; that is, for each nucleus an unweighted mean of the  $G_L$  measurements was extracted. This mean is used to calculate  $H$  via Eq. (1). The electromagnetic matrix elements for  $2_1^+$  states are taken from the compilation by Raman *et al.* [43]. The corresponding matrix elements for  $3_1^-$  states are taken from Spear's compilation [2].

For  $2_1^+$  states, the average value of  $H$ ,  $\langle H \rangle$ , for the 37 nuclei listed is 1.20, and the standard deviation is 0.44. For  $3_1^-$  states,  $\langle H \rangle$  for the 30 nuclei listed (1.15) is similar, but the standard deviation (0.35) is somewhat smaller. These results can be seen qualitatively in Figs. 5 and 6: The  $H$  values for  $3_1^-$  states are slightly less scattered, while there are more very small ( $<0.7$ )  $H$  values in the  $2_1^+$  state plot.

In his survey of  $3_1^-$  states using  $(p, p')$  results supplied by authors, Spear obtained a result of 0.97 for  $\langle H \rangle$  for all even-even nuclei, and a result of 1.01 with a standard deviation of 0.36 when only  $A > 20$  nuclei were considered. If the author-supplied results (as listed by Spear) are considered only for  $A \geq 40$  nuclei (Spear lists 47 such nuclei), then a mean value of 1.05 and a standard deviation of 0.36 are obtained. As a result, our consistent

TABLE II. Results of analysis of  $(p, p')$  data for  $3_1^-$  states.

| Nucleus          | $E_{\text{beam}}$ (MeV) | Ref. | $\beta_3^a$ | $G_L$ (W.u.) <sup>b</sup> | Nucleus           | $E_{\text{beam}}$ (MeV) | Ref. | $\beta_3^a$ | $G_L$ (W.u.) <sup>b</sup> |
|------------------|-------------------------|------|-------------|---------------------------|-------------------|-------------------------|------|-------------|---------------------------|
| <sup>40</sup> Ar | 29.6                    | 6    | 0.280       | 10.4                      | <sup>70</sup> Ge  | 22.0                    | 24   | 0.265       | 29.4                      |
| <sup>40</sup> Ar | 35.1                    | 6    | 0.288       | 11.0                      | <sup>72</sup> Ge  | 22.0                    | 24   | 0.240       | 24.1                      |
| <sup>40</sup> Ar | 16.9                    | 7    | 0.340       | 15.3                      | <sup>74</sup> Ge  | 22.0                    | 24   | 0.150       | 9.4                       |
| <sup>40</sup> Ar | 14.1                    | 7    | 0.347       | 16.0                      | <sup>76</sup> Ge  | 22.0                    | 24   | 0.150       | 9.4                       |
| <sup>40</sup> Ca | 17.3                    | 7    | 0.480       | 37.7                      | <sup>88</sup> Sr  | 20.2                    | 25   | 0.170       | 17.1                      |
| <sup>40</sup> Ca | 35.0                    | 8    | 0.362       | 21.4                      | <sup>88</sup> Sr  | 19.5                    | 26   | 0.170       | 17.1                      |
| <sup>40</sup> Ca | 30.0                    | 8    | 0.380       | 23.6                      | <sup>90</sup> Zr  | 25.0                    | 27   | 0.190       | 23.6                      |
| <sup>40</sup> Ca | 25.0                    | 8    | 0.371       | 22.5                      | <sup>90</sup> Zr  | 18.8                    | 28   | 0.180       | 21.2                      |
| <sup>40</sup> Ca | 40.0                    | 8    | 0.353       | 20.4                      | <sup>92</sup> Zr  | 40.0                    | 29   | 0.160       | 16.8                      |
| <sup>40</sup> Ca | 14.6                    | 7    | 0.552       | 49.9                      | <sup>94</sup> Zr  | 19.4                    | 30   | 0.190       | 23.6                      |
| <sup>42</sup> Ca | 22.9                    | 9    | 0.278       | 12.6                      | <sup>92</sup> Mo  | 15.0                    | 31   | 0.190       | 26.1                      |
| <sup>50</sup> Ti | 40.0                    | 11   | 0.160       | 5.1                       | <sup>94</sup> Mo  | 25.6                    | 32   | 0.190       | 26.1                      |
| <sup>50</sup> Ti | 17.5                    | 12   | 0.209       | 8.6                       | <sup>94</sup> Mo  | 15.0                    | 31   | 0.170       | 20.9                      |
| <sup>50</sup> Ti | 18.2                    | 13   | 0.195       | 7.5                       | <sup>96</sup> Mo  | 25.6                    | 32   | 0.210       | 31.8                      |
| <sup>52</sup> Cr | 17.5                    | 14   | 0.200       | 9.4                       | <sup>96</sup> Mo  | 15.0                    | 31   | 0.200       | 28.9                      |
| <sup>52</sup> Cr | 40.0                    | 11   | 0.140       | 4.6                       | <sup>98</sup> Mo  | 15.0                    | 31   | 0.205       | 30.3                      |
| <sup>52</sup> Cr | 17.5                    | 12   | 0.170       | 6.8                       | <sup>98</sup> Mo  | 14.7                    | 33   | 0.210       | 31.8                      |
| <sup>54</sup> Fe | 40.0                    | 15   | 0.094       | 2.4                       | <sup>100</sup> Mo | 25.6                    | 32   | 0.200       | 28.9                      |
| <sup>54</sup> Fe | 17.9                    | 13   | 0.136       | 5.1                       | <sup>100</sup> Mo | 15.0                    | 31   | 0.220       | 34.9                      |
| <sup>56</sup> Fe | 17.5                    | 14   | 0.290       | 23.3                      | <sup>116</sup> Sn | 24.5                    | 34   | 0.170       | 29.6                      |
| <sup>58</sup> Ni | 39.7                    | 18   | 0.190       | 11.6                      | <sup>118</sup> Sn | 24.5                    | 34   | 0.180       | 33.1                      |
| <sup>58</sup> Ni | 17.8                    | 41   | 0.190       | 11.6                      | <sup>120</sup> Sn | 24.5                    | 34   | 0.155       | 24.6                      |
| <sup>60</sup> Ni | 19.0                    | 16   | 0.200       | 12.8                      | <sup>120</sup> Sn | 30.0                    | 35   | 0.190       | 36.9                      |
| <sup>60</sup> Ni | 17.8                    | 41   | 0.180       | 10.4                      | <sup>122</sup> Sn | 24.5                    | 34   | 0.155       | 24.6                      |
| <sup>62</sup> Ni | 19.0                    | 16   | 0.220       | 15.5                      | <sup>124</sup> Sn | 24.5                    | 34   | 0.140       | 20.0                      |
| <sup>64</sup> Zn | 15.0                    | 19   | 0.240       | 21.2                      | <sup>138</sup> Ba | 30.0                    | 36   | 0.112       | 16.1                      |
| <sup>64</sup> Zn | 30.0                    | 22   | 0.180       | 11.9                      | <sup>140</sup> Ce | 30.0                    | 37   | 0.106       | 15.5                      |
| <sup>66</sup> Zn | 22.0                    | 20   | 0.260       | 24.9                      | <sup>144</sup> Sm | 30.0                    | 38   | 0.150       | 35.4                      |
| <sup>68</sup> Zn | 22.0                    | 23   | 0.240       | 21.2                      | <sup>208</sup> Pb | 40.0                    | 39   | 0.110       | 33.3                      |
| <sup>68</sup> Zn | 50.0                    | 42   | 0.220       | 17.8                      | <sup>208</sup> Pb | 35.0                    | 40   | 0.127       | 44.4                      |
| <sup>70</sup> Zn | 22.0                    | 23   | 0.210       | 16.2                      |                   |                         |      |             |                           |

<sup>a</sup>The errors for  $\beta_2$  are 7.5%.

<sup>b</sup>Calculated from  $\beta_2$  using Eq. (3). The errors for  $G_L$  are 15%.

reanalysis has yielded a somewhat higher value of  $\langle H \rangle$  (1.15), but has not changed the standard deviation of  $H$  at all. This suggests that the distribution of  $H$  values results not from variations in the methods of analysis, but instead from errors in measuring absolute cross sections and from real physical effects in the nuclei which have been studied. The scatter of results from different  $(p, p')$  experiments on the same nuclei certainly suggests

that considerable experimental errors exist. For example, results for the  $3_1^-$  state of <sup>40</sup>Ca range from 21.4 to 49.9 W.u. (see Table II).

However, the more important reason for the differences in  $G_L$  and electromagnetic results is that protons and neutrons generally do not contribute equally to the mass multipole moments induced by nuclear excitations, and different probes [such as  $(p, p')$  and Coulomb excitation]

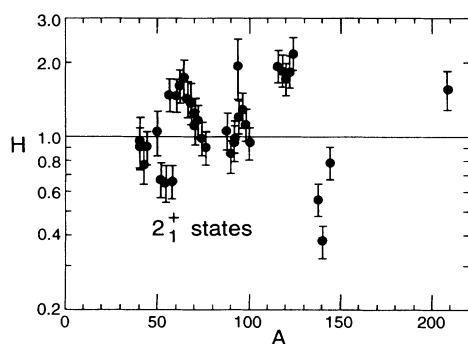


FIG. 5.  $H$  values for  $2_1^+$  states of the nuclei analyzed here.

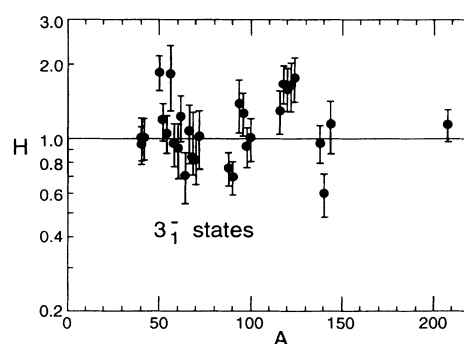


FIG. 6.  $H$  values for  $3_1^-$  states of the nuclei analyzed here.

have different sensitivities to the protons and neutrons [3]. If  $N > Z$  in a nucleus (as is the case for almost all nuclei considered here) and if the amplitudes of the vibrations of the proton and neutron fluids are equal (as they would be for an isoscalar vibration), then the neutrons would give a larger contribution to the mass multipole moment. Furthermore, electromagnetic probes measure only the charge (or proton) multipole moment, while  $(p, p')$  is three times more sensitive to target neutrons than to target protons at the energies discussed here [3]. Consequently, the variations from  $H = 1$  that are observed here are not surprising. These effects are examined in more detail in Sec. IV.

#### IV. COMPARISON OF NEUTRON AND PROTON MULTIPOLE MATRIX ELEMENTS

When the  $2_1^+$  and  $3_1^-$  states of an even-even nucleus are discussed as collective excitations, it is usually assumed that they are isoscalar. However, it has been shown [3] that differences can occur between the amplitudes of the motions of protons and neutrons in  $2_1^+$  states. Such a difference is measured in a particular nucleus by comparing the matrix elements connecting the  $2_1^+$  state to the ground state as seen by two different experimental probes. Madsen, Brown, and Anderson [44] found that the comparison of a low-energy (10–50 MeV)  $(p, p')$  result to an electromagnetic matrix element is particularly sensitive to a difference in the amplitudes of proton and neutron motion.

In this section, we use the  $(p, p')$  information extracted in the present study to look for the differences in proton and neutron motion in both  $2_1^+$  and  $3_1^-$  states. We will follow the prescription of [3] for this analysis. This analysis focuses on determining the ratio of the transition matrix elements  $M_n$  (for neutrons) and  $M_p$  (for protons), where the matrix elements are given by

$$M_{n(p)} = \left\langle J_f \left\| \sum_{n(p)} r_i^\lambda Y_\lambda(0_i) \right\| J_i \right\rangle, \quad (3)$$

where the sum is over the neutrons (protons) in the nucleus. This microscopic quantity can be related to the macroscopic oscillation amplitudes  $\beta_{n(p)}$  for neutrons (protons) via the equation

$$M_n/M_p = (N\beta_n)/(Z\beta_p). \quad (4)$$

If the amplitudes of the neutron and proton fluid oscillations are equal ( $\beta_n = \beta_p$ ), then  $M_n/M_p = N/Z$ . This result corresponds to the usual isoscalar collective model picture. If  $M_n/M_p > N/Z$ , then the amplitude of the neutron oscillations is larger than that of the protons. When  $M_n/M_p < N/Z$ , the proton oscillations are larger.

To calculate  $M_n/M_p$  from  $(p, p')$  and electromagnetic data, we must specify how each probe interacts with the nucleons in the nucleus. The electromagnetic probes interact only with the protons. The scattered protons interact with the neutrons in the target approximately three times more strongly than with the target protons

[3]. Bernstein, Brown, and Madsen [3] use this information to calculate  $M_n/M_p$  with the equation

$$\frac{\delta(F)}{\delta_p} = \frac{1 + (b_n^F/b_p^F)(M_n/M_p)}{1 + (b_n^F/b_p^F)(N/Z)}, \quad (5)$$

where  $\delta(F)$  is the deformation length ( $=\beta R$ ) from a probe  $F$  [in our case  $(p, p')$  at low energies],  $\delta_p$  is the electromagnetic deformation length ( $=\beta_{em}R$ ), and  $b_n^F/b_p^F$  is the ratio of the external field interactions strengths of the probe  $F$  with neutrons and protons in the target nucleus. For low-energy  $(p, p')$ ,  $b_n^F/b_p^F$  is approximately 3, and that is the value we use in our analysis. Equation (4) gives

$$\frac{M_n}{M_p} = \frac{b_p^F}{b_n^F} \left[ \frac{\delta(F)}{\delta_p} \left( 1 + \frac{b_n^F}{b_p^F} \frac{N}{Z} \right) - 1 \right]. \quad (6)$$

For the present analysis, we set  $\delta(F) = \beta_{(p,p')}(1.17 \text{ fm})A^{1/3}$ , since the radius of the real central part of the Becchetti-Greenlees optical potential is  $R = (1.17 \text{ fm})A^{1/3}$ . To set  $\delta_p$ , we use the prescription

$$\delta_p = \frac{R_0}{Z(3+L)} [B(EL)(4\pi)(2L+1)]^{1/2} \quad (7)$$

with  $R_0 = (1.20 \text{ fm})A^{1/3}$ . The quantity  $(M_n/M_p)/(N/Z)$ , which is equal to 1 for an isoscalar excitation, is plotted in Figs. 7 and 8 for  $2_1^+$  and  $3_1^-$  states, respectively.

From the shell-model picture of nuclei it might be ex-

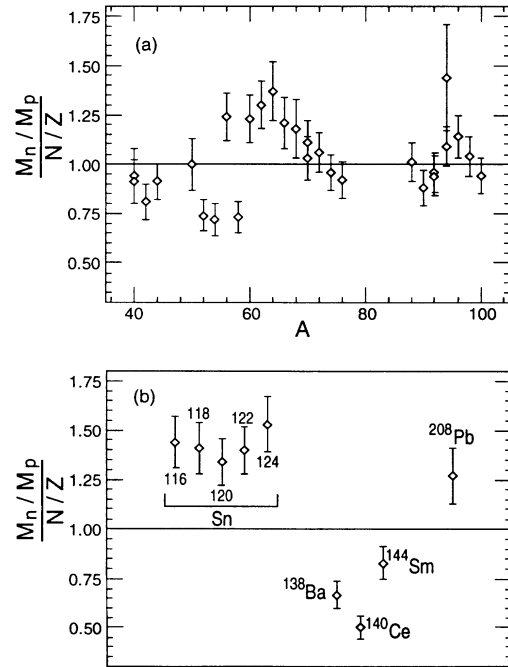


FIG. 7. (a)  $(M_n/M_p)/(N/Z)$  values for  $2_1^+$  states of the nuclei analyzed here in the mass range  $40 \leq A \leq 100$ . (b)  $(M_n/M_p)/(N/Z)$  values for the  $2_1^+$  states of  $^{116, 118, 120, 122, 124}\text{Sn}$ ,  $^{138}\text{Ba}$ ,  $^{140}\text{Ce}$ ,  $^{144}\text{Sm}$ , and  $^{208}\text{Pb}$ .

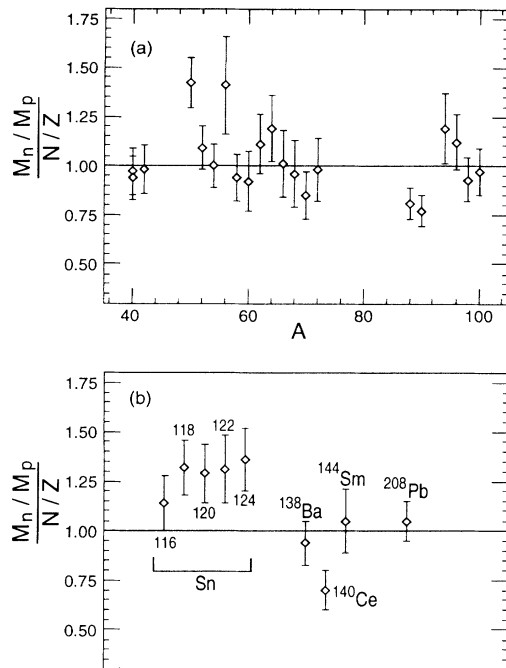


FIG. 8. (a)  $(M_n/M_p)/(N/Z)$  values for  $3_1^-$  states of the nuclei analyzed here in the mass range  $40 \leq A \leq 100$ . (b)  $(M_n/M_p)/(N/Z)$  values for the  $3_1^-$  states of  $^{116,118,120,122,124}\text{Sn}$ ,  $^{138}\text{Ba}$ ,  $^{140}\text{Ce}$ ,  $^{144}\text{Sm}$ , and  $^{208}\text{Pb}$ .

pected that the most significant differences between proton and neutron contributions to  $2_1^+$  and  $3_1^-$  states would occur in single-closed-shell (SCS) nuclei, in which the nucleus has a closed neutron shell and valence protons, or a closed proton shell and valence neutrons. A shell-model calculation for a closed neutron shell nucleus that has valence protons which assumes an inert core would predict that the  $2_1^+$  and  $3_1^-$  states would consist entirely of excitations of the valence protons. In a real nucleus, the core is not inert and core polarization occurs; however, schematic model calculations [3] predict that the excitations of the valence protons would dominate the  $2_1^+$  states of closed neutron shell nuclei. (The opposite situation is predicted to occur in closed proton shell nuclei which have valence neutrons.)

An examination of the  $2_1^+$  state results in Fig. 7 shows two groups of nuclei for which the predictions of the schematic model calculations are dramatically confirmed. The Sn isotopes, with their closed proton shells, have  $(M_n/M_p)/(N/Z)$  values systematically above 1.00, indicating that the  $2_1^+$  states are dominated by neutrons, as would be expected from the schematic model. The closed

neutron shell  $N = 82$  isotones  $^{138}\text{Ba}$ ,  $^{140}\text{Ce}$ , and  $^{144}\text{Sm}$  lie well below 1.00, once again confirming the prediction of the schematic model that protons should dominate their  $2_1^+$  states. The other SCS nuclei for which we have results do not yield results as systematically significant as these two groups.

There are no corresponding schematic model calculations of  $3_1^-$  states of which we are aware; however, it is plausible that neutrons (protons) would dominate the  $3_1^-$  states of closed proton (neutron) shell nuclei. Among the  $3_1^-$  state results shown in Fig. 8, the most interesting group of nuclei in this regard is the Sn isotopes. The  $(M_n/M_p)/(N/Z)$  values for these nuclei are once again systematically larger than 1.00, indicating the dominance of neutrons in the  $3_1^-$  states. However, among the nuclei shown in Fig. 8, the  $3_1^-$  states seem to be generally more isoscalar [with  $(M_n/M_p)/(N/Z)$  closer to 1] than the  $2_1^+$  states. This would suggest that core polarization is generally stronger for  $3_1^-$  states than for  $2_1^+$  states. A theoretical investigation of core polarization in  $3_1^-$  states would be interesting.

## V. CONCLUSIONS

We have performed a reanalysis of a large amount of  $(p, p')$  data for  $2_1^+$  and  $3_1^-$  states of even-even  $A \geq 40$  nuclei at energies between 14 and 50 MeV using a consistent procedure involving coupled-channels calculations and Becchetti-Greenlees optical model parameters [5]. We have found that variations in the method of analysis do *not* cause the differences which often occur between  $(p, p')$  and electromagnetic results. Instead, these differences may be traced to experimental errors and physical effects in the nucleus.

By analyzing both the  $(p, p')$  and electromagnetic results, we have been able to compare the motions of protons and neutrons in the  $2_1^+$  and  $3_1^-$  states of nuclei studied here. Differences in the proton and neutrons oscillations occur in the  $2_1^+$  states of the Sn isotopes and  $N = 82$  isotones, and in the  $3_1^-$  states of the Sn isotopes. Overall, it appears that the differences between proton and neutron motions are smaller in  $3_1^-$  states than in  $2_1^+$  states in the nuclei studied here. This result suggests that the core polarization effect is stronger in  $3_1^-$  states than in  $2_1^+$  states.

## ACKNOWLEDGMENTS

We acknowledge useful discussions with D. Robson and R.H. Spear. This work was supported by the National Science Foundation and the State of Florida.

- [1] A. M. Bernstein, in *Advances in Nuclear Physics*, edited by M. Baranger and E. Vogt (Plenum, New York, 1969), Vol. 3, p. 325ff.
- [2] R. H. Spear, *At. Data Nucl. Data Tables* **42**, 55 (1988).
- [3] A. M. Bernstein, V. R. Brown, and V. A. Madsen, *Comments Nucl. Part. Phys.* **11**, 203 (1983).
- [4] P. D. Kunz, University of Colorado report (unpublished).

- [5] F. D. Becchetti and G.W. Greenlees, *Phys. Rev.* **182**, 1190 (1969).
- [6] R. de Leo, S. Micheletti, M. Pignanelle, and M. N. Harakeh, *Phys. Rev. C* **31**, 362 (1985).
- [7] W. S. Gray, R. A. Kenefick, and J. J. Krauhaar, *Nucl. Phys.* **67**, 542 (1965).
- [8] C. R. Gruhn, T. Y. T. Kuo, C. J. Maggiore, H. McManus,

- F. Petrovich, and B. M. Freedom, Phys. Rev. C **6**, 915 (1972).
- [9] J. C. Bane, J. J. Kraushaar, B. W. Ridley, and M. M. Stautberg, Nucl. Phys. **A116**, 580 (1968).
- [10] R. J. Peterson and D. M. Perlman, Nucl. Phys. **A117**, 185 (1968).
- [11] B. M. Freedom, C. R. Gruhn, T. Y. T. Kuo, and C. J. Maggiore, Phys. Rev. C **2**, 166 (1970).
- [12] H. O. Funsten, N. R. Roberson, and E. Rost, Phys. Rev. **134**, B117 (1964).
- [13] W. S. Gray, R. A. Kenefick, and J. J. Kraushaar, Nucl. Phys. **67**, 565 (1965).
- [14] R. J. Peterson, Ann. Phys. **53**, 40 (1969).
- [15] M. P. Fricke, E. E. Gross, and A. Zucker, Phys. Rev. **163**, 1153 (1967).
- [16] S. F. Eccles, A. F. Lutz, and V. A. Madsen, Phys. Rev. **141**, 1067 (1966).
- [17] G. S. Mani, Nucl. Phys. **A157**, 471 (1970).
- [18] T. Stovall and N. M. Hinz, Phys. Rev. **135**, B330 (1964).
- [19] M. J. Throop, Y. T. Cheng, A. Goswami, O. Nalcioglu, D. K. McDaniels, L. W. Swenson, N. Jarmie, J. H. Jett, P. A. Lovoi, D. Stupin, G. G. Ohlsen, and G. G. Salzmann, Nucl. Phys. **A283**, 475 (1977).
- [20] J. Jabbour, L. H. Rosier, B. Ramstein, R. Tamisier, and P. Avignon, Nucl. Phys. **A464**, 260 (1987).
- [21] R. R. Johnson and G. D. Jones, Nucl. Phys. **A122**, 657 (1968).
- [22] W. H. Tait and V. R. W. Edwards, Nucl. Phys. **A203**, 193 (1973).
- [23] J. Jabbour, L. H. Rosier, B. Ramstein, R. Tamisier, and P. Avignon, Nucl. Phys. **A464**, 287 (1987).
- [24] L. H. Rosier, J. Jabbour, B. Ramstein, P. Avignon, and R. Tamisier, Nucl. Phys. **A453**, 389 (1986).
- [25] J. Picard, O. Beer, A. el Behay, P. Lopato, Y. Terrien, G. Vallois, and R. Shaeffer, Nucl. Phys. **A128**, 481 (1969).
- [26] M. M. Stautberg, J. J. Kraushaar, and B. W. Ridley, Phys. Rev. **157**, 977 (1967).
- [27] L. T. van der Bul, H. P. Blok, J. F. A. van Heinen, and J. Blok, Nucl. Phys. **A393**, 173 (1983).
- [28] W. S. Gray, R. A. Kenefick, J. J. Kraushaar, and G. R. Satchler, Phys. Rev. **142**, 735 (1966).
- [29] R. de Swiniarski, D-L. Phan, G. Bagieu, and H. V. Geramb, Can. J. Phys. **57**, 540 (1979).
- [30] M. M. Stautberg and J. J. Kraushaar, Phys. Rev. **151**, 969 (1966).
- [31] A. F. Lutz, D. W. Keikikinan, and W. Bartolini, Phys. Rev. C **4**, 934 (1971).
- [32] E. Fretwurst, G. Lindstrom, K. F. von Reden, V. Riech, S. J. Vasilijev, P. P. Zarubin, O. M. Knyazkov, and I. N. Kuchtina, Nucl. Phys. **A468**, 247 (1987).
- [33] Y. Awaya, K. Matsuda, T. Wada, N. Nakanishi, S. Takeda, and S. Yamaji, J. Phys. Soc. Jpn. **33**, 881 (1972).
- [34] O. Beer, A. el Behay, P. Lopato, Y. Terrien, G. Vallois, and K. K. Seth, Nucl. Phys. **A147**, 326 (1970).
- [35] S. A. Fulling and G. R. Satchler, Nucl. Phys. **A111**, 81 (1968).
- [36] D. Larson, S. M. Austin, and B. H. Wildenthal, Phys. Rev. C **9**, 1574 (1974).
- [37] J. D. Sherman, D. L. Hendrie, and M. S. Zismar, Phys. Rev. C **15**, 903 (1977).
- [38] J. H. Barker and J. C. Hiebert, Phys. Rev. C **4**, 2256 (1971).
- [39] A. Scott and M. P. Fricke, Phys. Lett. **20**, 654 (1966).
- [40] W. T. Wagner, G. M. Crawley, G. R. Hammerstein, and H. McManus, Phys. Rev. C **12**, 757 (1975).
- [41] O. M. Jarvis, B. G. Harvey, D. L. Hendrie, and J. Mahoney, Nucl. Phys. **A102**, 625 (1967).
- [42] V. E. Lewis, M. Calderbank, N. K. Ganguly, and M. P. Fricke, Nucl. Phys. **A117**, 673 (1968).
- [43] S. Raman, C. H. Malarkey, W. T. Milner, C. W. Nestor, Jr., and P. H. Stelson, At. Data Nucl. Data Tables **36**, 1 (1987).
- [44] V. A. Madsen, V. R. Brown, and J. D. Anderson, Phys. Rev. C **12**, 1205 (1975).